# Prototyping of an Olfactory Display supported by CFD Simulations

Marco Rossoni[1] , Marina Carulli[2] , Monica Bordegoni[3] and Giorgio Colombo[4]

[1]Politecnico di Milano, marco.rossoni@polimi.it
[2]Politecnico di Milano, marina.carulli@polimi.it
[3]Politecnico di Milano, monica.bordegoni@polimi.it
[3]Politecnico di Milano, giorgio.colombo@polimi.it

Corresponding author: Marco Rossoni, marco.rossoni@polimi.it

**Abstract.** Olfactory Displays are devices used to generate and deliver scented air that is eventually smelled by the users. As the literature reports, their development and evaluation mostly rely on experimental activities based on a "trial-and-error" approach, which prevents a comparative analysis of designed solutions and their technical performances, thus leading to prototypes with low potential to become future products. In this paper, an innovative framework embedding Computational Fluid Dynamics (CFD) simulations for designing, prototyping and testing new Olfactory Displays is proposed. After presenting the framework, the paper illustrates the settings for a multi-phase CFD analysis based on Discrete Particles Modeling for simulating olfactory displays. The design of a new wearable olfactory display is presented, detailing all the steps of the framework. A first architecture is devised, and an initial set of simplified 2D multi-phase CFD simulations has been used to propose possible improvements. A new design has been developed, and a 3D CFD simulation has been run to predict its performance. A set of experiments has been conducted to test the real prototypes and compare the performance with the one predicted by the simulations. The experimental results are in good accordance with the simulations, which have proven their effectiveness in improving the design of the olfactory displays.

**Keywords:** Virtual and Physical Prototyping, Rapid Prototyping, CFD, Olfactory Display
**DOI:** https://doi.org/10.14733/cadaps.2023.174-189

## 1 INTRODUCTION

The sense of smell has been mostly neglected in Western society for a long time. Among the different sensory modalities, smell has long been underestimated, especially compared to other senses, such as vision and hearing. Nevertheless, the smell is one of the most primordial senses in humans [4], and odors directly stimulate the oldest brain areas (the limbic lobe) involved in memory and emotional processing. It has only been a few years since research has highlighted the importance of

this sense for perceiving the environment around us, enriching the users' experiences, and making them more engaging.

Researchers are increasingly committed to studying methods and tools to exploit the use of the sense of smell in products and services to improve their User Experience. The User Experience is strictly linked to the user interaction with objects at physical, perceptual, and cognitive levels. This means that it also includes the design of multisensory experiences that also satisfy sight, touch, hearing, and smell senses [7]. In addition, in recent years, studies on digital olfaction have advanced in many directions. Moreover, several prototypes of devices delivering smells, named Olfactory Displays, have been developed and tested.

Olfactory Displays are devices based on several technologies used to generate and deliver scented air that is eventually smelled by the users [16]. The olfactory display generates scented air from odorous materials kept in a stocked form (liquid, soaked in porous materials, gelled, etc.) by using techniques like heating, airflow vaporization, atomization, and transmits it to the human olfactory organ through delivery systems, as pipes, directed airflow, and direct injection [16]. The development of an olfactory display is based on the characteristics of the olfactory process. The smell is a chemical media, and still, there is no consensus on the classification of "primary" scents. Therefore, according to the scenarios to develop, olfactory displays and applications, including smells, use a limited number of smell components. In the last decade, several scent generation and delivery methods have been developed and used to implement various applications (such as [8]). The authors have developed applications based on the use of odors to stimulate users' attention and make the reading experience more immersive [5], improve the quality of the users' experience of artworks [6], and improve the immersiveness of Extended Reality experiences. Olfactory displays are not technologically mature since many technical issues remain unsolved related to olfaction, such as adaptation, detection, and recognition thresholds. Some companies have proposed commercial versions of the devices for personal use. Recent examples are the Vaqso device (https://vaqso.com/), the Olorama scents generator (https://www.olorama.com), and the Feelreal device (https://feelreal.com/).

All research prototypes and commercial devices have several limitations regarding the number of odors they can produce, their size and wearability, and their performances. For these reasons, the commercial devices have not penetrated the market yet. The main underlying reason is related to the inherent complexity of these devices because the smell is a chemical sense, and there is still no complete comprehension of all its mechanisms and features. In addition, many studies in the literature report experimental activities based on a "trial-and-error" approach, which prevents a comparative analysis of designed solutions and their technical performances, thus leading to prototypes with low potential to become future products.

The work presented in this paper aims at advancing the know-how for designing and implementing olfactory displays by proposing an innovative framework. The paper illustrates the framework, describes its main steps, and presents a case study to demonstrate its use in designing a new wearable olfactory display. The paper describes in detail the Computational Fluid Dynamics simulation of the designed Olfactory Display, which is one of the framework steps since it has proven to be particularly effective in identifying the best design solutions.

## 2    RELATED WORKS

Olfactory Displays (OD) are devices controlled by computers that generate and deliver scented air, eventually smelled by the users [16]. The development of an Olfactory Display is based on the characteristics of the olfaction process. Because humans perceive smells through the air, the two main functions of an Olfactory Display are scent generation and scent delivery. For both, different technologies have been developed. The scent generation is the process where the odor to be delivered is effectively generated. The generation can be obtained in different ways, but it always involves the presence of the odor stocked in some form. Scent delivery is the delivery process for conveying scented air from the generator to the user's nose [16].

The process of generating odors depends on the physical status of essences, which usually are in liquid form, and then soaked in porous materials, encapsulated, or gelled. Several techniques can be used for generating scented molecules from the liquid: for example, it is possible to use airflow-based vaporization, heating, airflow-based atomization, direct atomization - piezoelectric method, and ultrasonic atomization. On the other side, it is possible to deliver odors by using, for example, natural diffusion/convection, wind, vortex ring, tubes, and direct injection.

In addition, the smell is a chemical sense, and there is still no complete comprehension of all its mechanisms and features. Firstly, there is no consensus on the classification of "primary" smells (as in the case of colors for visual perception), and a general and commonly shared classification of odors has not been developed. Therefore, according to the scenarios to design, olfactory displays and applications, including smells, use a limited number of smell components. Secondly, an important issue is the non-linearity of the smell (a modification of the intensity of the stimulus can result in a qualitative change in the subjective sensation). Finally, olfactory perception and classification depend on several factors, like age, sex, gender, nationality, background, etc.

In the last decade, several scent generation and delivery methods have been developed and used to implement various applications [8]. Many research projects have used these technologies for developing ubiquitous and personal ODs for specific aims. For instance, Kim et al. [13] designed and developed an OD based on a container of temperature-responsive hydrogel that can have reversible changes between sol and gel. Yamada et al. [25] developed wearable ODs to present the spatiality of smell in an outdoor environment. Narumi et al. [17] developed a "Pseudo-gustatory" OD for creating a gustatory sensation. Hirota et al. [10] developed olfactory displays for multi-sensory theatres. Moreover, some of the authors have developed applications based on the use of odors to stimulate users' attention and make the reading experience more immersive [5], improve the quality of the users' experience of artworks [6], for products evaluation [3], to improve the drivers' attention level [4] and to improve the immersiveness of Extended Reality experiences.

Olfactory displays are not technologically mature since many technical issues related to olfaction remain unsolved, such as adaptation, detection, and recognition thresholds. Some companies have proposed commercial versions of the devices for personal use. Recent examples are the Vaqso device (https://vaqso.com/), the Olorama scents generator (https://www.olorama.com), and the Feelreal device (https://feelreal.com/).

Even though odorant airflow plays a crucial role in the performance of an olfactory display [22], few authors have taken Computational Fluid Dynamics (CFD) simulations into account to predict the behavior of the prototypes and the influence of the device architecture. Matsukura et al. [14] have performed a CFD simulation to understand how odors generated from an olfactory display spread in an open environment. A similar approach has been proposed in [12] and [2]. In both cases, the purpose of performing CFD simulation was to understand how odor concentration changes in space and time in a room: the olfactory display was modeled as an odor source without considering the actual geometry. The results of the simulations were compared with experimental sessions involving humans: through qualitative metrics, the prediction of the CFD analysis matches what the testers reported. To the authors' knowledge, the integration of fluid dynamics to improve the architecture of the olfactory display has not yet been investigated in the literature.

The simulation of an olfactory display requires a multi-phase fluid domain to be considered: the odor particles emitted from the device interact with the air in the environment, determining the overall performance of the prototype. Simulating a multi-phase fluid domain through Computational Fluid Dynamics is still challenging due to the complexity of the phenomena involved. Several methods have been implemented to simulate the inertial response and the interactions among the phases [21]. Broadly speaking, two different numerical frameworks can be used to account for multiple phases within the domain. The Euler-Lagrange solves the continuum phase (i.e., the air in our case) using Navier-Stokes equations, while the second phase (i.e., the mist in our case) consists of discrete particles. The Euler-Euler approach considers both phases as continuous. A comprehensive overview of the governing equations can be found in [21]. The selection of the modeling framework strongly depends on the phenomena and the flow regimes under investigation.

No applications on olfactory display are reported in the literature, while Computational Fluid Dynamics methods are widely used in droplet/aerosol research [28, 24].

For this reason, generic simulations of sprays and industrial atomizers have been explored to select the most suitable strategy to address the scope of this research. Among the Euler-Euler approaches, the Volume of Fluid (VOF) is one of the most used for investigating phenomena involving complex free boundaries configuration [11], like a dam break, and the steady or transient tracking of any liquid-gas interface. Through a single set of momentum equations, the method can track the volume fraction of each phase within the domain, the droplets' generation mechanisms, and the liquid-gas interface. This method has been widely used to simulate plasma sprays [18] or the spray condition in pressure-swirl atomizers [9]. Despite this approach can capture fine details regarding the spray formation, it is demanding from a modeling and computational point of view.

On the contrary, the Lagrange-Euler simulation approaches account for a secondary discrete phase while solving transport equations for the continuous phase. The Discrete Particle Method (DPM) [23] is one of the most representative implementations of this class of approaches. In the specific case, the particles are dispersed in the fluid phase, and heat and mass exchange, collisions, break-up, and turbulence can be considered. The mist generated by a mesh atomizer is composed of droplets of liquid water suspended in the environment (i.e., air) [26]: it falls in the category of a gas-liquid "droplet flow" where the dispersed flows (i.e., the mist) volume fraction is much lower than the continuum phase (i.e., the air) [1, page 565]. As the scope of CFD in this work is to predict how the mist propagates throughout the prototype channels and in the environment after passing through the mesh atomizer, the Discrete Particle Method is the one that best suits the purpose of this research. For this type of problem, the DPM approach is suggested [1].

## 3   THE DESIGN FRAMEWORK

The framework aims at supporting designers and researchers in designing new Olfactory Displays by suggesting the most appropriate methods and tools to obtain the optimal design solution. The framework is based on experimental activities and integrates parametric modeling, Computational Fluid Dynamics (CFD) simulation, and rapid prototyping technologies to continuously evaluate possible alternative solutions and rapidly converge to a final optimal one.

In fact, among the several problems related to the design and development of these devices is the lack of precise guidelines about the techniques that can be used for releasing odorous substances, the form in which these odorous substances are preserved, i.e., liquid or solid, the number of odorous substances to use, the duration of the release of the odorous substance, etc. These elements, and many others, are fundamental in the design of devices to allow and optimize the perception of odors. This is related to the significant variability of parameters to be managed in the context of an Olfactory Display project, which often makes the design based on "trial-and-error" and personal experience, but also to the great difficulty of objectively verifying, through experimental activities, the technical performances of new Olfactory Displays. Regarding this point, the instruments necessary to carry out precise experimental tests exist, but they are costly and difficult to find. Therefore, most designers find it difficult or even impossible to use them.

For these reasons, the olfactory display design framework here proposed aims, in the early stages, to guide designers and researchers in defining the technological requirements and solutions to be used concerning the chosen scenarios of use and, in a second phase, to support the validation of the designed solutions through comparative experimental activities, which consists of comparing data obtained with real prototypes and those obtained with CFD simulations.

In particular, the framework consists of the following six steps, which are shown in figure 1:

1   Definition of Requirements (based on the specific application)
2   Selection of the components for the generation and delivery of smells from a library of technological solutions reported in the literature [16]
3   Design of the Olfactory Display architecture and shape

4    Experimental activities, including parametric modeling, CFD simulation, and rapid prototyping

5    Comparative tests and evaluation of the data collected in the tests

6    Refinement of the Olfactory Display architecture and shape

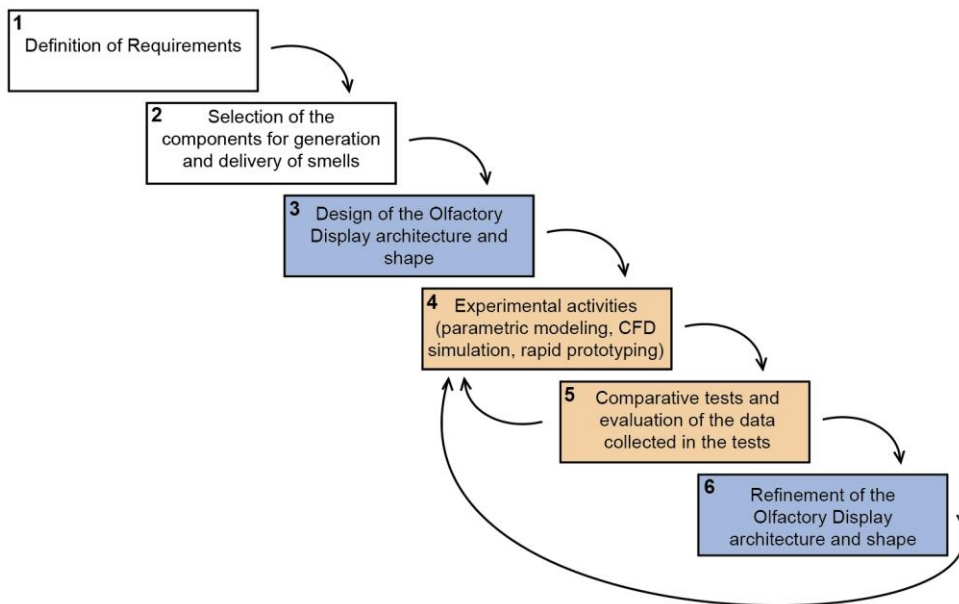Steps from 4 to 6 should be repeated in a loop until the desired design solution is achieved.



**Figure 1:** The structure of the framework.

An experimental case study has been conducted to evaluate the proposed design framework. The following sections describe all the activities and results of this design process.

## 4    CASE STUDY

The definition of the scenario of use of the olfactory display has important repercussions on all the design choices that will then be made in the following steps.

As a first case study to evaluate the experimental framework it was decided to design and develop a wearable olfactory display to be used indoors and outdoors, to relax in stressful moments, improve moods and evoke positive emotions.

The users should be able to wear and bring the device with them at any time. The device must release three different smells to relax when needed, which can be chosen and reloaded by the user. The device must be controllable through an app.

Based on these features of the use scenario, the *Requirements definition* step (step 1) has been carried out. First, the feature related to the wearability of the device implies that the olfactory display must be portable (in a bag or a backpack) and wearable (like a necklace). It must be light and small so that the user can comfortably carry it with him/her, and must have a battery (possibly rechargeable). From an analysis of wearable devices, it was decided that the device must weigh a maximum 400 gr.

Because the device can be used in open places, the device must have a system to properly and effectively deliver the scented air to the user's nose.

The device must deliver three smells, even simultaneously, which can be easily reloaded or replaced by the users according to their preferences. In particular, the number of odors has been defined to meet both a good range of flexibility for the user and reasonable weight and size of the device and duration of the odors' cartridges. In general, even if the number of odors could be considered small, the possibility for the user to recharge or replace them according to her/his preferences will allow great flexibility of use.

In the step 2 of the framework, the "*Selection of the components for the generation and delivery of smells from a library of technological solutions reported in the literature*" has been carried out. In this phase, based on the defined requirements, the selection of the most suitable techniques for scent generation and scent delivery and the form in which the odorous substances are stored have been defined. In particular, as a first step, some technologies have been discarded as inadequate. Since the device is wearable, those technologies that involve the use of heat, which could be annoying or dangerous for the user if worn, and technologies that involve large or heavy systems have been discarded. On the contrary, particular attention has been paid to lightweight technologies that require little energy to operate. At the end of this analysis, the *piezoelectric mesh atomizer* technology has been selected. It allows for producing and delivering a sparse scented mist (air with suspended droplets) starting from water in which one or more essences have been diluted. This technology has been selected as the most appropriate for wearable devices since it allows for small size, lightweight, and a high degree of safety.

Subsequently, in step 3, the architecture and shape of the Olfactory Display have been defined. Figures 2 and 3 present the Olfactory Display architecture and form, respectively. Each piezoelectric mesh atomizer has been connected to a single cartridge containing scented water to avoid mixing smells. Besides, two separate parts have been created to allow cartridges to be refilled and replaced, one containing the scented water and the other the electronics. Experimental studies have shown that the mechanism stops working and requires the user's intervention if the cartridge is placed under the piezoelectric mesh atomizer after a few cycles. In fact, in this layout, the water level goes down and a small cylinder of porous cotton is used to transmit the scented water up to the piezoelectric mesh atomizer. However, the water quantity is not enough for the correct functioning of the piezoelectric mesh atomizer, and a frequent water refill is needed. Therefore, it was decided to place the piezoelectric mesh atomizers under the cartridge. Immediately after the atomizer, a U-shaped channel was inserted, which allows the scented mist to be conveyed upwards, i.e., towards the user's nose.
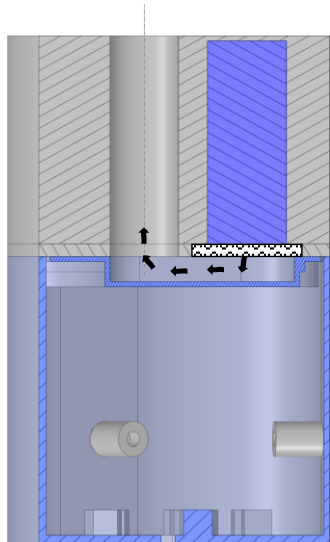


**Figure 2:** Architecture of the designed Olfactory Display.

**Figure 3:** Parametric 3D model of the designed Olfactory Display.

In step 4, the parametric model of the Olfactory Display was developed. It was used to manufacture the first physical prototype created using rapid prototyping techniques (figure 4). In addition, preliminary CFD simulations of the digital prototype have been performed.



**Figure 4:** Physical prototype of the designed Olfactory Display.

Comparative tests of the real prototype have been performed in step 5. Some operating problems of the real prototype were detected that concerned the flow of the scented mist through the output channel and the speed of the same. Consequently, it was decided to simulate the integration of a fan to help the mist escape the Olfactory Display, thus decreasing the probability for the mist to condensate on the channel walls and for the particles to coalesce. As the introduction of a fan introduces drawbacks from a wearability point of view, a new Olfactory Display was designed, where it has been changed the architecture of the channel and the position of the mesh atomizer (step 6).

So, steps from 4 to 6 have been repeated in a loop until the desired design solution was achieved. These activities will be described in the following sections.

## 4.1 CFD Simulations

A set of CFD simulations have been set up and performed in Ansys Fluent 2022 R1. As previously discussed, the DPM model has been adopted. The fluid pressure and velocity fields are computed by solving the Navier-Stokes equations, while the tracking of discrete phase (the droplets in this case) is derived from the calculated flow field. The particles can act as passive stream (one-way coupling) or interact with the fluid flow (two-ways coupling): in our case, the interaction with the continuous phase has been enabled. The droplet collision and coalescence are tracked in the simulation using the O'Rourke algorithm [19]. The analysis has been set as transient, and the effect of gravity has been enabled as it can have an impact on the trajectory of the particle. Concerning the turbulence model, the literature [15] shows that it strongly affects the numerical stability, but there is no preferred choice. The realizable k-ε model has been reported as one of the most stable and accurate in spray applications [20]. For this reason, it has been used for all the simulations reported in this paper.

The first set of simulations has been performed to investigate the behavior of the architecture. In this case, a 2D multiphase transient simulation is used to simulate the behavior of the mist between the piezoceramic mesh atomizer and the atmosphere. As CFD simulations for multiphase flows are quite challenging, the fluid domain has been simplified to obtain its 2D projection on the midplane of the device. Despite reducing the domain of a 3D volume to a 2D planar surface may lead to inaccuracies in turbulence-related quantities, it makes the simulation convergence easier to reach, especially considering the kind of models employed to account for the particles' behavior. On the other hand, a 2D domain still allows us to draw some considerations that can be beneficial for prototyping such a device. The fluid domain (Figure 2) has been discretized with quadrilateral-dominant quadratic elements of 0,1 mm length inside the fluid region. An inflation layer control has been added to all the walls to catch the rapid changes in the flow's variables close to the walls and to get the appropriate y+ value for the turbulence model selected (i.e., the k-ε requires y+ values between 100 and 300). Six layers are generated with a growing ratio of 1,2, and a first-layer thickness of 10 μm. On the edge where $m_p$ is applied, 100 elements have been imposed because the number of particles injected in the volume will depend on the number of elements on the injection edge. The mesh parameters just described have been decided after a mesh independency study.

The air has been modeled as a compressible fluid with a density of 1,225 kg/m3. The particles are injected from the surface where the mesh atomizer is supposed to be (see Figure 5). The material assigned to the particle is liquid water while the diameter is 10 μm [27], and their behavior is set to "inert". The injection lasts for 0.5 s with a total mass flow rate of 20 g/s (as prescribed by the atomizer specifications), and a discrete random walk model is employed to predict the dispersion of particles due to turbulence in the fluid phase using a stochastic method. One of the assumptions of the DPM model is that an inert particle obeys the force balance and, therefore, its velocity equates to the one of surrounding flow.

For this reason, the mass flow rate of air at the inlet ($m_p$) has been initially set equal to the particles' mass flow rate (20 g/s). The rest of the boundaries are stationary walls. Regarding the boundary condition for the discrete phase, the inlets and the outlet allow the particle to escape the domain while the walls trap the particle (i.e., the trajectory tracking is terminated when the particle collides with the wall). The last boundary conditions allow the simulation to account (to a certain extent) for the condensation and coalescence phenomena of the particles on the wall that has been observed experimentally. The pressure at the outlet of the domain ($P_{out}$) has been set at 0 Pa, as a 101325 Pa operating pressure has been set at 48 mm. The pressure-velocity scheme has been set as coupled, the spatial discretization for the momentum, the turbulence energy, and the dissipation rate as second-order upwind and transient formulation as second-order implicit. The time step for the simulation is 5 ms, and 200 steps have been computed for a total simulation time of 1 s.
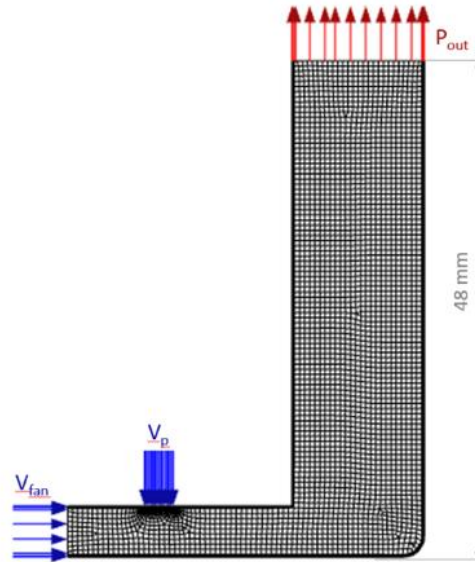
**Figure 5:** Particle residence time for the simulation.

A total of 12 different simulations have been run to understand the impact of having different inlet velocities and the magnitude of the inlet boundary conditions changes according to the values reported in Table 1. The setup described above has remained unchanged for all the 12 simulations performed. $V_{fan}$ is the velocity inlet condition for the airflow coming from the eventual fan.

| Simulation # | mp [g/s] | $V_{fan}$ [m/s] | Simulation # | mp [g/s] | $V_{fan}$ [m/s] |
|:---:|:---:|:---:|:---:|:---:|:---:|
| S1 | | 0 | S7 | | 0 |
| S2 | | 0,1 | S8 | | 0,1 |
| S3 | 20 | 0,2 | S9 | 40 | 0,2 |
| S4 | | 0,3 | S10 | | 0,3 |
| S5 | | 0,4 | S11 | | 0,4 |
| S6 | | 0,5 | S12 | | 0,5 |

**Table 1:** Velocity inlet magnitudes of the particle (Vp) and the fan (Vfan) for the 12 simulations.

## 4.2 Results on the First Set of CFD Simulations

To summarize the results of the simulations, the time for the first particle to escape the fluid domain and the percentage of escaped particles have been tracked. For the simulations S1 and S7, where the fan is deactivated, the particles struggle to reach the outlet in the time prescribed by the simulation (1 s): none of the particles escapes in S1, while only the 20% of them leave the domain in S7. When the piezo is deactivated after 0.5 s, the fluid flow does not have enough inertia to push the particle out of the channel. This situation is, in fact, what can be experienced by testing the device experimentally: all the droplets coalesce, and a puddle of liquid can be found on the bottom. As soon as the fan gets activated, the "efficiency" of the device improves. Figure 6 shows the particle residence time for S1 and S4 at the end of the simulation, while Figure 7 summarizes the results for all the other simulations.
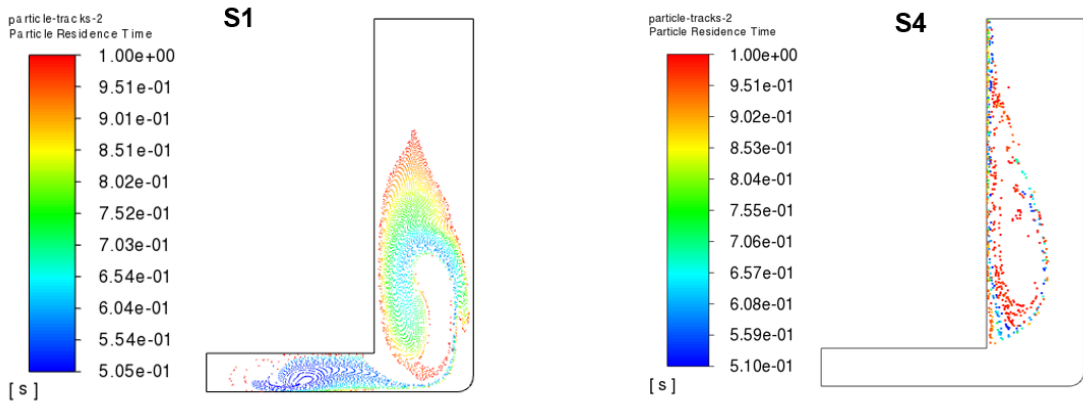
**Figure 6:** Particle residence time for the simulation S1 (on the left) and S4 (on the right).
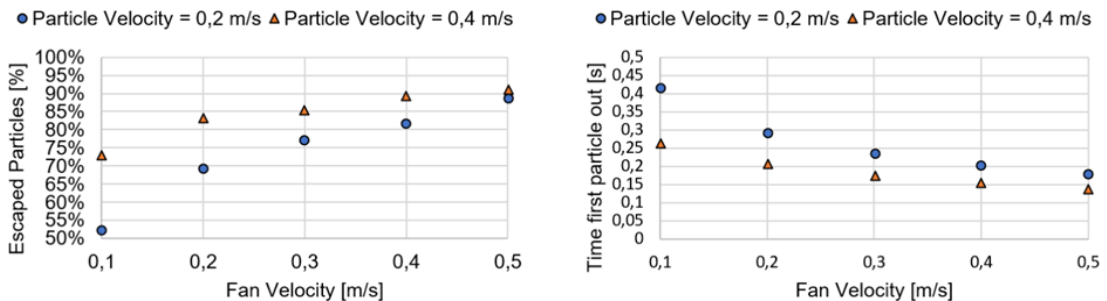


**Figure 7:** Escaped particle percentage and time for the first particle to escape the volume.

The two main conclusions from the data presented here are: (i) the fan is an essential component for the prototype for the defined architecture as it improves the percentage of particles that can escape the volume, and (ii) there is no need to push the fan at the maximum speed since the marginal gain becomes low at the expenses of increasing the power consumption of the Olfactory Display.

## 4.3    Revised Architecture and Second Set of CFD Simulations

Even though the introduction of a fan can improve the overall performance of the olfactory display from a fluid dynamic perspective, one of the requirements for the prototype is to be wearable and lightweight. Adding such a device would have side effects, jeopardizing the wearability of the final prototype. For example, the mass of a 1'' (25x25x10mm) generic fan can weigh between 15 and 25 grams, the power consumption is around 3 W, requires a battery of 12 V, and moves about 1 dm$^3$/s at 1500 rpm with a noise level of 20db. It would be helpful to avoid it while retaining the functionality of the prototype. For this reason, in step 6 of the framework, the architecture of the Olfactory Display has been revised, exploiting both the experiments and the simulations. The latter indicates that, without a fan (S1 and S7, Table 1), the piezoelectric mesh atomizer cannot push the air out of the channel: the experiment validated this result and made clear that the problem is, on top of the reduced mass flow rate, the tendency of the mist to coalesce on the walls of the channels. Therefore, the prototype architecture has been rethought as follows: (i) the mesh atomizer has been moved to the end of the channel, and (ii) the output channel has been shortened. With this new configuration, the authors aimed to obtain a continuous water flow under the piezoelectric mesh atomizer to feed

it and reduce the mist coalescence on the walls of the output channel. Figure 8.a shows the new configuration of the Olfactory Display.
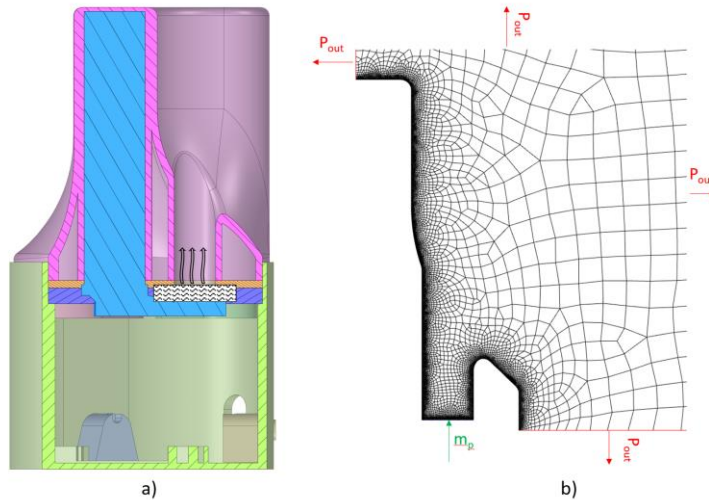


**Figure 8**: a) section of the prototype, the blue part corresponds to the water while the wavy part represents the atomizer. B) 2D mesh and boundary conditions.

The setup of the simulation for the new architecture is identical to the one presented before, except for the mesh and the boundary conditions. A detail of the new mesh is shown in Figure 8.b. The fluid domain is now a volume representing the environment, and it extends for about 300 mm in each direction. The pressure at the outlet of the domain ($P_{out}$) has been set at 0 Pa, as a 101325 Pa operating pressure has been set at the y-position of the mesh atomizer. The value of the mass flow rate has been kept unchanged (0,2 g/s) as well as all the settings for the walls. In this case, the maximum y coordinate for the particles has been tracked, as it is a metric easy to compare with the experimental sessions (described below). Figure 9 shows the dispersed particles after 0.5 s from the activation of the atomizer: this time corresponds to the maximum extension of the mist. The simulation time has also been extended to 2s but, after 0.5s, the particle's inertia dissipates, and the effect of the gravity prevails. The maximum height predicted by the 2D simulation is 212 mm.

As the dispersion of the particles in the environment is dominated by turbulence and the approximation of 3D volume to a 2D planar domain may lead to inaccuracies in turbulence-related quantities, a 3D simulation has been performed.

Figure 10 shows the 3D fluid domain, whose dimensions surround the prototype walls by 300x300x300 mm. The solving schemas and the boundary conditions have been kept unchanged. The fluid domain has been discretized with polyhedral elements of 1 mm length inside the fluid region. A local refinement has been imposed at the inlet and the portion of the channel pertaining to the prototype. Here, the average mesh size has been set at 0.2mm, and the proximity and curvature controls have been enabled to ensure a smooth transition with the rest of the domain. An inflation layer control has been added to all the walls to catch the rapid changes in the flow's variables close to the walls and to get the appropriate y+ value for the turbulence model selected (i.e., the k-ε requires y+ values between 100 and 300). Six layers are generated with a growing ratio of 1,2, and a first-layer thickness of 10 μm. The final mesh counts 110000 nodes. The mesh parameters just described have been decided after a mesh independency study. The time-step has been fixed at 1 ms, and a total of 1000 steps has been computed.
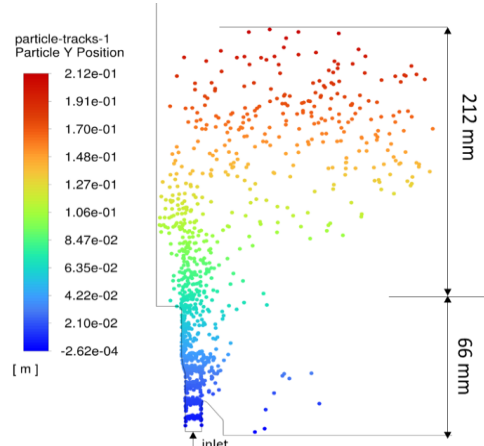
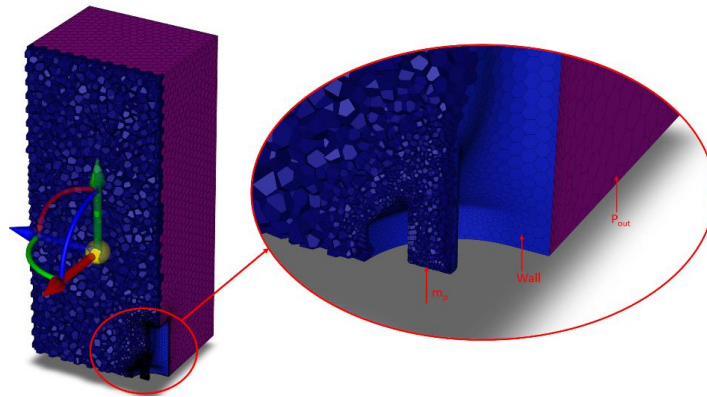**Figure 9**: Particle Y position after 0.5 seconds.
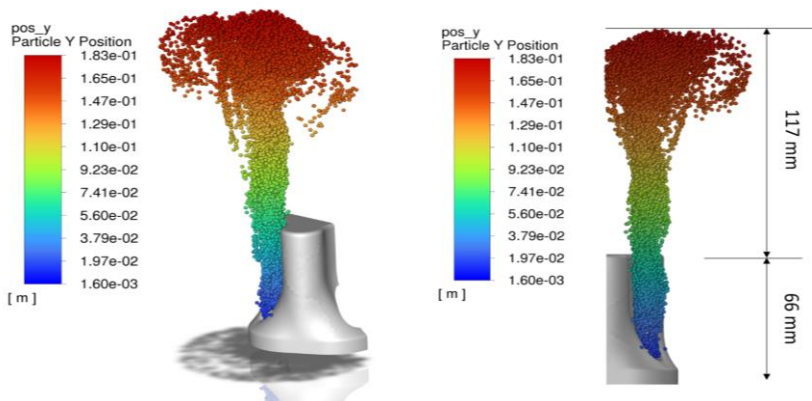


**Figure 10**: Cut-out of the 3D mesh.



**Figure 11**: Cut-out of the 3D mesh particle Y position after 0.5 seconds for the 3D simulation. On the left is an isometric view; on the right, the front view for comparison with Figure 9

Figure 11 shows the Y-position of the particle at 0.5s from the activation of the atomizer. The maximum height achieved by the particles, according to the 3D simulation, is 117 mm from the top surface of the prototype.

## 4.4 Comparative Experimental Activities and Discussion

Experimental activities with the real prototype have been performed to compare the results obtained with the CFD simulations. Specifically, the prototype has been opened, and a single cartridge of the prototype has been filled in with 13 gr of water. Then, the lower and the upper part of the prototype have been attached, and the piezoelectric mesh atomizer linked with the water cartridge has been activated (see Figure 12). It has been observed that the scented mist created by the atomizer reaches more than 100 mm for a duration of about 10 minutes.



**Figure 12**: Experimental activities with the real prototype.

Although the 3D simulations are more accurate than a 2D approximation, the computational resources needed to obtain the results are not comparable. All the simulation described here has been performed on a PC equipped with an Intel Xeon E5-2650 v4, and 64 Gb RAM: for all the simulation, 20 cores have been allocated. With these settings, the 2D domain has been solved in 15-20 minutes on average, while the 3D simulation took 25 hours to complete. This is mainly due to the size of the meshes that for the 3D discretization is intrinsically bigger (10k elements and 110k elements for the 2D and 3D domain respectively) and the time step needs to ensure the converge of the numerical model (1 ms and 5ms for the 2D and 3D domain respectively). Despite the 2D simulation cannot be used to precisely define the dispersion of the particles in the environment, they are still useful to have a rough idea of what is going on in the domain: they have been proven very helpful to understand why the u-shaped device did not work properly and to decide how to improve the prototype. In general, they are a powerful tool to support fast design loops at an early stage of the development process. On the contrary, the 3D simulations can be used when the prototyping process is getting closer to the end: having reliable and accurate data at this point is important to optimize the performance of the final prototype.

## 5 CONCLUSIONS

The research work presented in this paper regards an innovative framework embedding CFD simulations for designing, prototyping, and testing new Olfactory Displays. The main purpose of the research is to support designers and researchers in designing new Olfactory Displays by suggesting the most appropriate methods and tools to obtain the optimal design solution.

To evaluate the proposed design framework, an experimental case study is presented, detailing all the framework steps. In particular, after the design phase, experiments with the real prototype and CFD simulations have been conducted, and the collected data have been compared.

Consequently, it is possible to say that CFD simulations can be successfully used to improve the design of the olfactory displays, overcoming the use of "trial-and-error" design approaches currently used as a common practice. It has been shown that researchers and designers can use the framework for defining novel design solutions for new olfactory displays and evaluating the technical performance by comparing the results of CFD simulations and experimental activities on real prototypes. This will make the design process much more robust and faster and allow us to obtain olfactory displays with even better performances.

Regarding the case study, some improvements will be carried out in the future. In particular, different architectures will be simulated to understand, considering the hardware available on the market, the best layout for the olfactory displays before the physical prototype is even produced. For the final validation of the framework, experimental sessions with real users should be conducted, and deeper investigation on CFD simulations for the olfactory display is needed. Although the simulations have been useful in driving the prototyping process, a thorough comparison between the numerical model and experimental results should be carried out. The evaluation of the CFD accuracy is essential to make use of the simulation results for optimization purposes, and, being able to predict how the odorants flow "behave" could also provide valuable insights into the olfactory perception research.

*Marco Rossoni*, http://orcid.org/0000-0003-2714-9043
*Marina Carulli*, http://orcid.org/ 0000-0003-2101-5474
*Monica Bordegoni*, http://orcid.org/ 0000-0001-9378-8295
*Giorgio Colombo*, http://orcid.org/ 0000-0002-9999-8960

## REFERENCES

[1] Ansys Fluent Theory Guide, 2022
[2] Ariyakul, Y.; Nakamoto, T.: Improvement of miniaturized olfactory display using electroosmotic pumps and SAW device. TENCON 2014 - 2014 IEEE Region 10 Conference, 2014. doi:10.1109/tencon.2014.7022484
[3] Bordegoni, M.; Carulli, M.: Evaluating Industrial Products in an Innovative Visual-Olfactory Environment, Journal of Computing and Information Science in Engineering, 16(3), 2016, 031004.
[4] Bordegoni, M.; Carulli, M.; Shi, Y.: Investigating the use of smell in vehicle-driver interaction, Proceedings of the ASME Design Engineering Technical Conference, Smart Innovation, Systems and Technologies, 65, 2016, 513-523.
[5] Bordegoni, M.; Carulli, M.; Shi, Y.; Ruscio, D.: Investigating the effects of odour integration in reading and learning experiences, Interaction Design and Architecture(s), 32, 2017, 104-125.
[6] Carulli, M.; Bordegoni, M.: Multisensory Augmented Reality Experiences for Cultural Heritage Exhibitions, Lecture Notes in Mechanical Engineering, 2020. https://doi.org/10.1016/j.cag.2021.10.001.
[7] Gallace, A.; Spence, C.: Multisensory design: Reaching out to touch the consumer, Psychology & Marketing, 28, 2011, 267-308.

[8]    Ghinea, G.; Ademoye, O.A.: Olfaction-enhanced multimedia: Perspectives and challenges. Multimedia Tools and Applications 55, 3, 2011, 601–626. https://doi.org/10.1007/s11042-010-0581-4

[9]    Gurakov, N.-I.; Zubrilin, I.-A.; Abrashkin, V.-Y.; Morales, M.-H.; Yakushkin, D.-V.; Yastrebov, V.-V.; Idrisov, D.-V.: Validation of the VOF method for liquid spray process simulation from a pressure-swirl atomizer, International Conference on Physics and chemistry of combustion and processes in extreme environments, 2020. https://doi.org/10.1063/5.0033854

[10]   Hirota, K.; Ito, Y.; Amemiya, T.; Ikei, Y.: Presentation of Odor in Multi-Sensory Theater, R. Shumaker (Ed.), VAMR/HCII-2013, 2013, 372–379.

[11]   Hirt, C.; Nichols, B.: Volume of fluid (VOF) method for the dynamics of free boundaries, Journal of Computational Physics, 39(1), 1981, 201–225. https://doi.org/10.1016/0021-9991(81)90145-5

[12]   Ishida, H.; Yoshida, H.; Nakamoto, T.: Introducing computational fluid dynamics simulation into olfactory display, Electrical Engineering in Japan, 177(1), 2011, 65–72. https://doi.org/10.1002/eej.21087

[13]   Kim, D.K.; Nishimoto, K.; Kunifuji, S.; Cho, Y.H.; Kawakami, Y.; Ando, H.: Development of Aroma-Card Based Soundless Olfactory Display, Electronics, Circuits, and Systems, 16th IEEE International Conference on., 2009.

[14]   Matsukura, H.; Ishida, H.: Incorporating Fluid Dynamics Considerations into Olfactory Displays, Human Olfactory Displays and Interfaces, 415–428. https://doi.org/10.4018/978-1-4666-2521-1.ch021

[15]   Montazeri, H.; Blocken, B.; Hensen, J.-L.: Evaporative cooling by water spray systems: CFD simulation, experimental validation and sensitivity analysis. Building and Environment, 83, 2015, 129–141. https://doi.org/10.1016/j.buildenv.2014.03.022

[16]   Nakamoto, T.: Human Olfactory Displays and Interfaces: Odor Sensing and Presentation, Information Science reference, 2013.

[17]   Narumi, T.; Nishizaka, S.; Kajinami, T.; Tanikawa, T.; Hirose, M.: Meta Cookie+: An Illusion-Based Gustatory Display, Virtual and Mixed Reality, 2011, 260-269.

[18]   Nasiri, M.-M.; Dolatabadi, A.; Moreau, C.: Modeling of liquid detachment and fragmentation during the impact of plasma spray particles on a cold substrate, International Journal of Heat and Mass Transfer, 189, 2022, 122718. https://doi.org/10.1016/j.ijheatmasstransfer.2022.122718

[19]   O'Rourke, P.-J.: Collective Drop Effects on Vaporizing Liquid Sprays. PhD thesis, Princeton University, Princeton, New Jersey, 1981.

[20]   Ruiz, J.; Martínez, P.; Martín, Í.; Lucas, M.: Numerical Characterization of an Ultrasonic Mist Generator as an Evaporative Cooler, Energies, 13(11), 2020, 2971. https://doi.org/10.3390/en13112971

[21]   Van Wachem, B.-G., Almstedt, A.E.: Methods for multiphase computational fluid dynamics, Chemical Engineering Journal, 96(1-3), 2003, 81–98. https://doi.org/10.1016/j.cej.2003.08.025

[22]   Wen, T.; Luo, D.; He, J.; Mei, K.: The Odor Characterizations and Reproductions in Machine Olfactions: A Review. Sensors, 18(7), 2018, 2329. https://doi.org/10.3390/s18072329

[23]   Xu, B.-H.; Yu, A.-B.: Numerical simulation of the gas-solid flow in a fluidized bed by combining discrete particle method with computational fluid dynamics, Chemical Engineering Science, 52(16), 1997, 2785–2809. https://doi.org/10.1016/s0009-2509(97)00081-x

[24]   Xu, P.-C.; Zhang, C.-M.; Wang, X.-C.: Numerical simulation for spatial distribution of water aerosol produced from nozzle spray and health risk related to Legionella pneumophila in spray scenarios, Water Research, 216, 2022, 118304. https://doi.org/10.1016/j.watres.2022.118304

[25]   Yamada, T.; Yokoyama, S.; Tanikawa, T.; Hirota, K.; Hirose, M.: Wearable Olfactory Display: Using Odor in Outdoor Environment, IEEE Virtual Reality Conf., 2006.

[26] Yan, Q.; Wu, C.; Zhang, J.: Effect of the Dynamic Cone Angle on the Atomization Performance of a Piezoceramic Vibrating Mesh Atomizer, Applied Sciences, 9(9), 2019, 1836. https://doi.org/10.3390/app9091836

[27] Yan, Q.; Sun, W.; Zhang, J.: Study on the Influencing Factors of the Atomization Rate in a Piezoceramic Vibrating Mesh Atomizer, Applied Sciences, 10(7), 2020, 2422. https://doi.org/10.3390/app10072422

[28] Yang, Y.; Wang, Y.; Song, B.; Fan, J.; Cao, Y.; Duan, M.: Transport and control of droplets: A comparison between two types of local ventilation airflows. Powder Technology, 345, 2019, 247–259. https://doi.org/10.1016/j.powtec.2019.01.008